Summary EMMI workshop
”Forward physics in ALICE 3”

Rainer Schicker
University Heidelberg

WE-seminar
Forward Physics and QCD at the LHC and the EIC

Oct 23-27, 2023

ALICE 3

Letter of intent for ALICE 3: arXiv: 2211.02491
A next-generation heavy-ion experiment

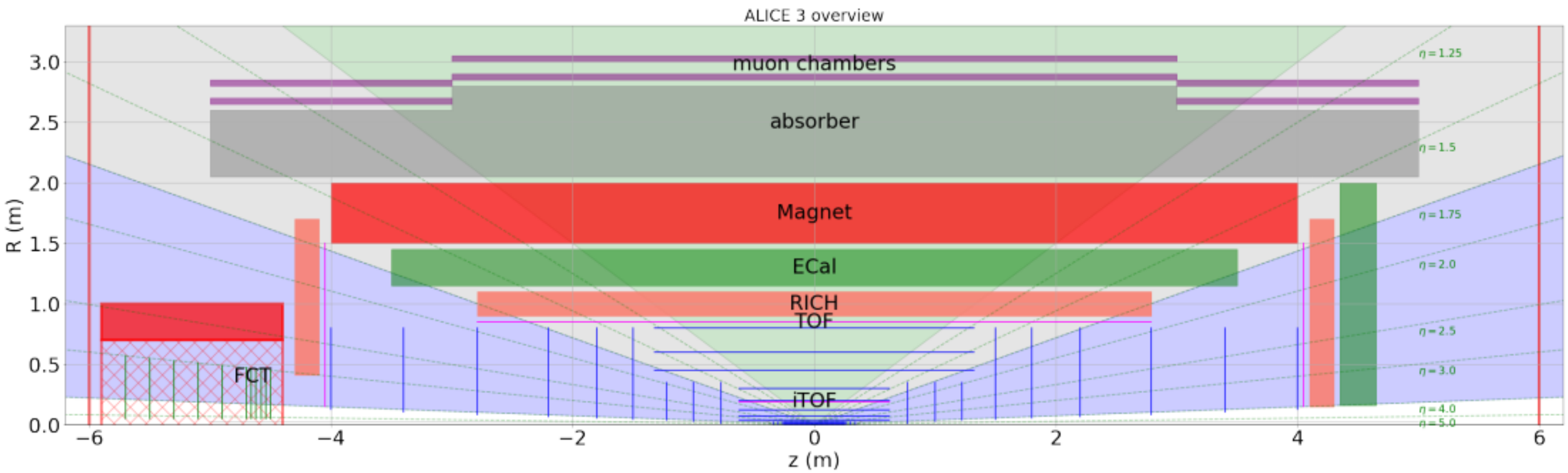

Figure 2: Longitudinal cross section of the ALICE 3 detector: The MAPS-based tracker is complemented by PID detectors (inner and outer TOF, RICH), all of which are housed in the field from a superconducting magnet system. In addition, the electromagnetic calorimeter (ECal), the muon identifier, and the Forward Conversion Tracker (FCT) are shown.

tracking central barrel: $|\eta| < 1.75$, forward $1.75 < |\eta| < 4$

PID: $\pi/K/p$ separation up to a few GeV$/c$

$\mathcal{L}_{\mathrm{pp}} = 3.0 \times 10^{32}$ cm^{-2}s^{-1}, $R_{max} = 24$ MHz, $\mu = 1.2$

EMMI Workshop Forward Physics in ALICE 3

ExtreMe Matter Institute EMMI

EMMI Workshop

Forward Physics in ALICE 3

Physikalisches Institut, Heidelberg University
October 18 - 20, 2023

Scientific topics:

- Proton-proton elastic and inelastic scattering
- Single and double diffractive proton dissociaton
- Exclusive production of dileptons, W^+W^- and $t\bar{t}$ pairs in pp collisions
- Exclusive production of dileptons and $c\bar{c}$ pairs in pA collisions
- Diffractive bremsstrahlung
- Soft photon production
- Gamma-proton cross section
- Vector meson photoproduction
- Gluon saturation in heavy-ion collisions

Organizers:

Alexandra Holten (secretary)
Piotr Lebiedowicz (co-chair)
Rainer Schicker (co-chair)
Martin Völkl

Information: www.gsi.de/emmi/workshops

Website: indico.cern.ch/event/1327118

More about EMMI: www.gsi.de/emmi

High β*-optics for ALICE

Pascal Hermes

CERN Beams Department
ABP-NDC

EMMI workshop on Forward Physics in ALICE 3
19.10.2023

What to expect from this contribution

- Beam dynamics: how are **beams guided and focused** in the LHC?
- How is the **final focus for the experiments** done?
- How can it be **optimized for forward physics**?
- What is unique about **ALICE & forward physics**?
- Which **constraints** do we have to respect?
- What are **concrete and reasonable options** that could be applied?

ALICE Optics '23

Upper proton luminosity limit in **ALICE: small β* not needed** (even luminosity levelling)

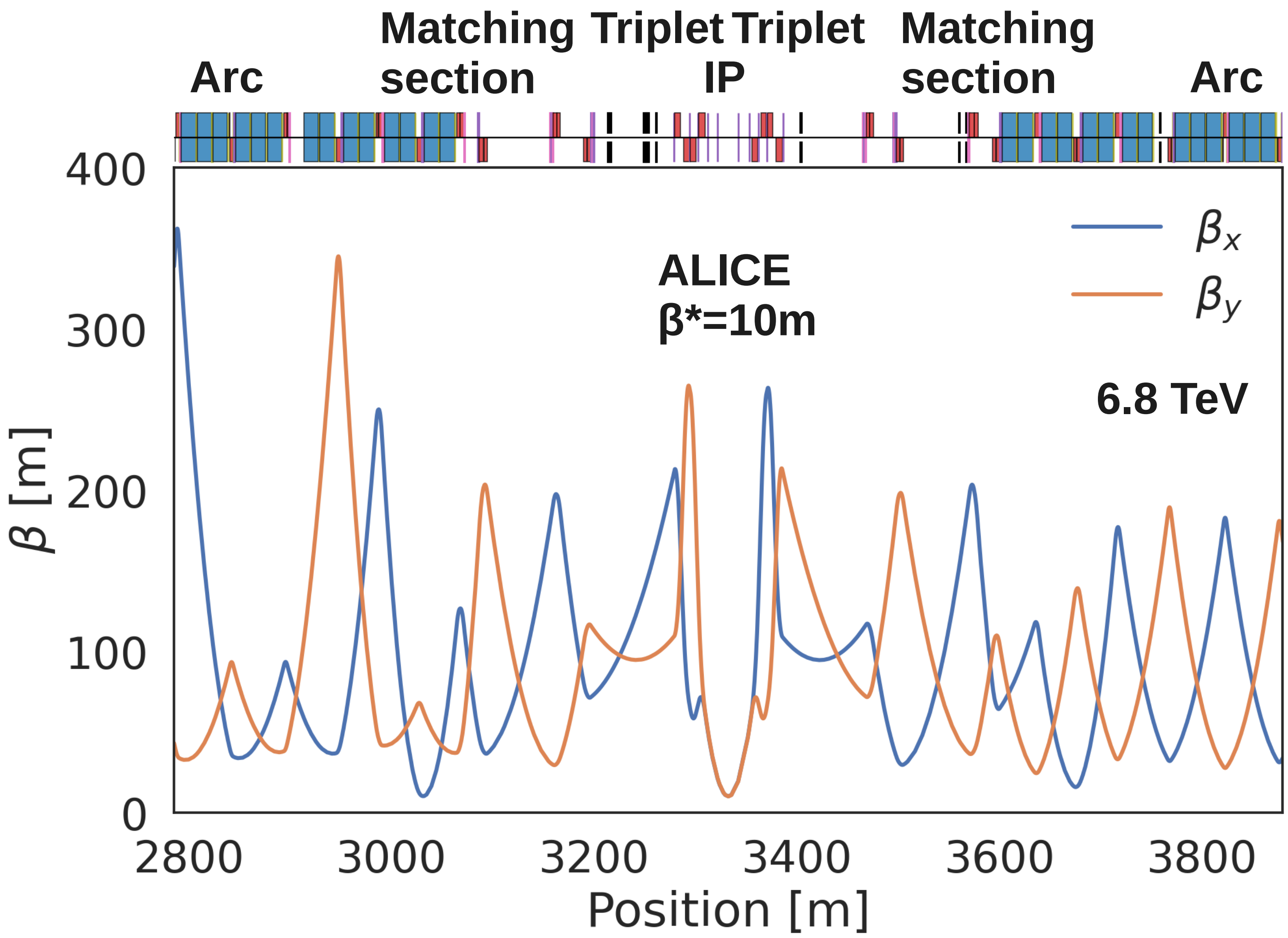

Global LHC Optics 2023

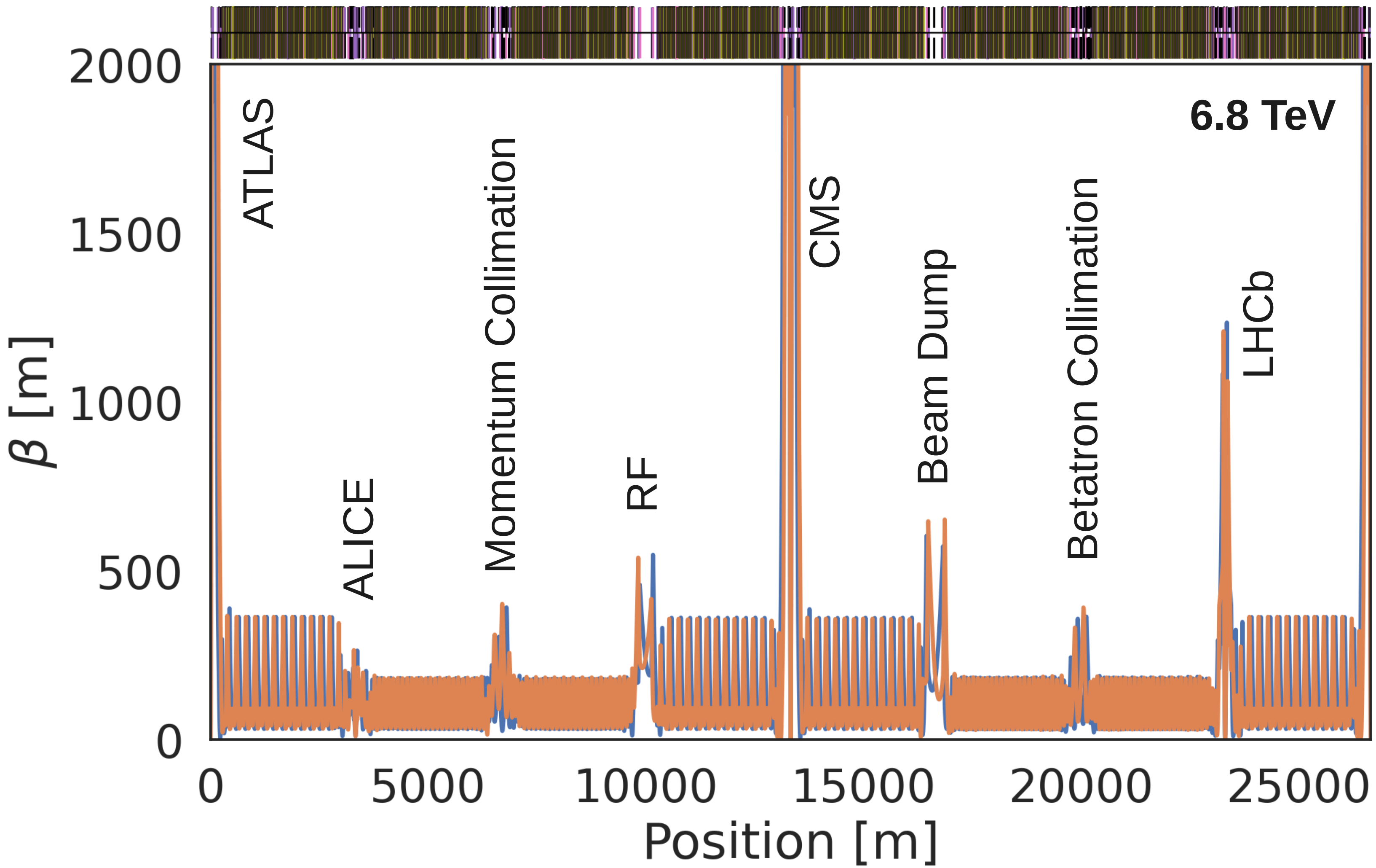

Perspective for ALICE

$$\mathcal{L} = \frac{n_B N_B^2 f_{\mathrm{rev}} \gamma}{4\pi \epsilon_N \beta^*} F$$

- ATLAS & CMS: high luminosity experiments
  - Main operational mode with squeezed beams (lowest possible β^*)
  - Very limited beam time available with large β^* to exploit forward detectors
- ALICE luminosity is levelled: no need for small β^*
  - If forward detectors were installed could operate nominally at larger β^*
  - What optics and β^* could be envisaged?

Assumed Roman Pot Positions

-220m -180m

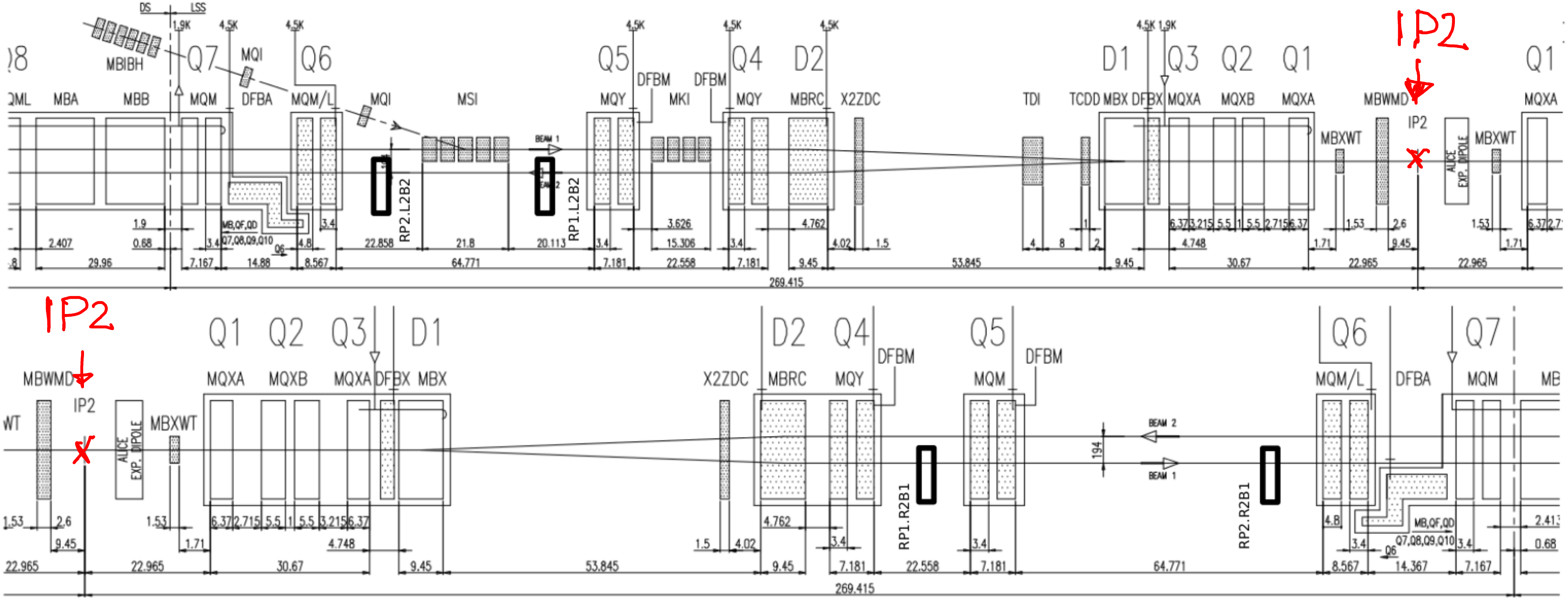

150m 220m

Optics constraints

- Largest possible β* in ALICE **compatible with high intensity operation**
- **Optical functions** at edges of insertion **must be matched** to arcs
- **Quadrupole currents** must be in certain range: $\mathbf{0.03 \leq k/k_{max} \leq 0.90}$
- **Symmetry** between B1 and B2 optics (double bore magnets with coupled circuits)
- **Tune** (number of betatron oscillations per turn) must be unchanged
- **Phase advance** between IP and second RP station close to π/2
- Enough **beam-beam separation** with the larger beams (25ns bunch spacing)
- **Aperture constraints** must be respected

Evolution with emittance (2013 study, LHC)

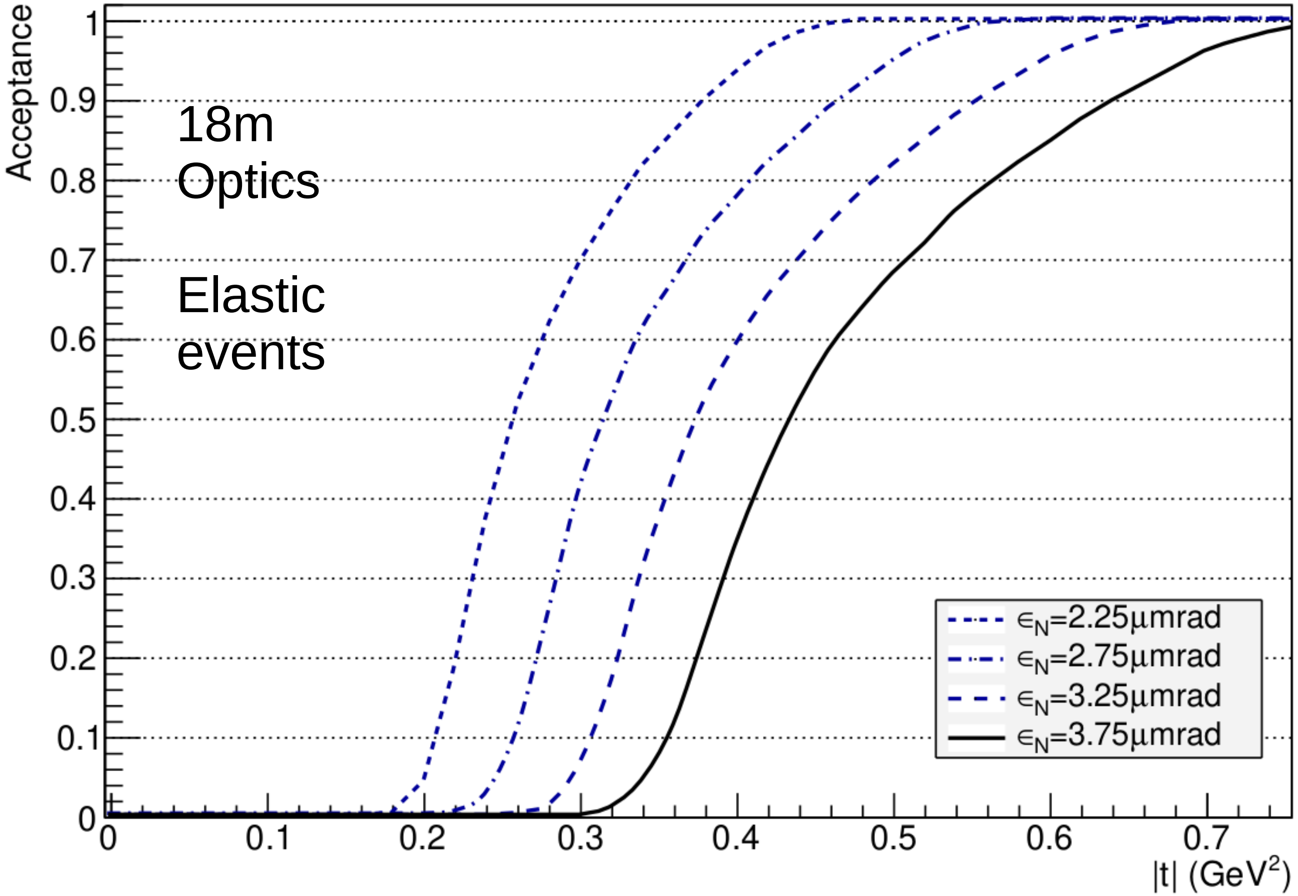

HL-LHC nominal
2.5µmrad

Evolution with beta (2013 study, LHC)

Elastic events

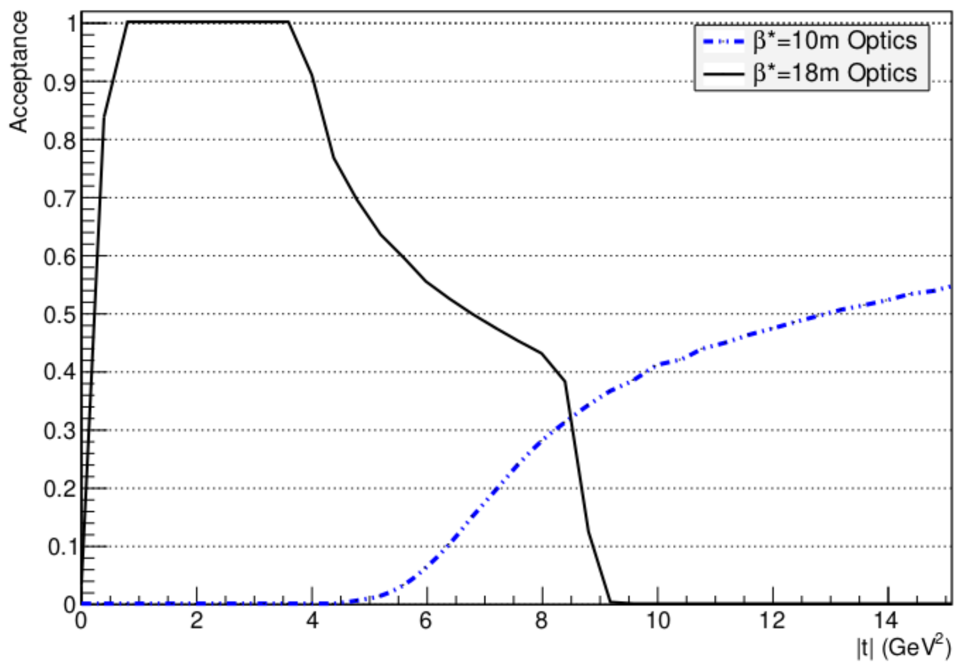

Elastic events

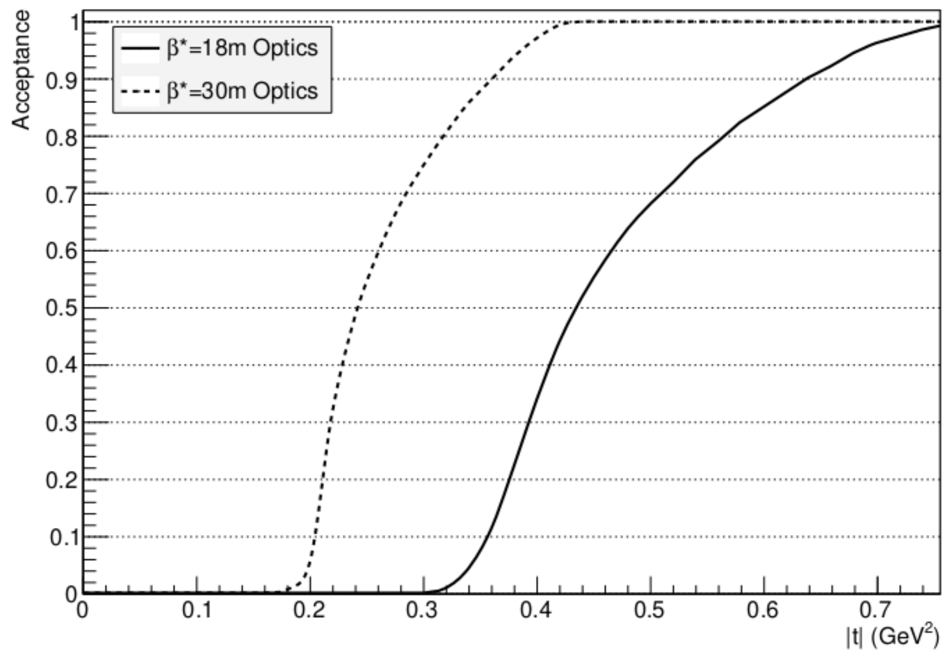

Dip-bump structures in pp elastic scattering and single diffractive dissociation

István Szanyi

in collaboration with László Jenkovszky

EMMI Workshop
Forward Physics in ALICE 3
18-20 October 2023, Heidelberg, Germany

Elastic pp scattering and single diffractive dissociation

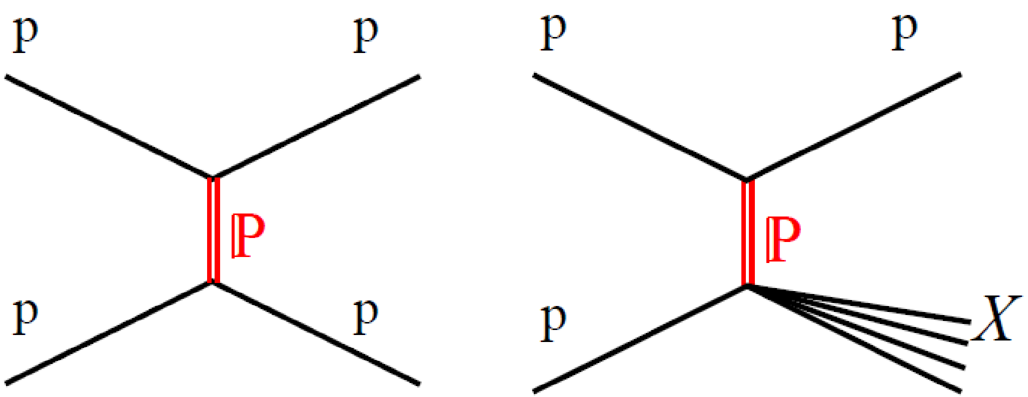

Leading order Pomeron exchange graph contributing to pp elastic scattering and to pp single diffractive dissociation

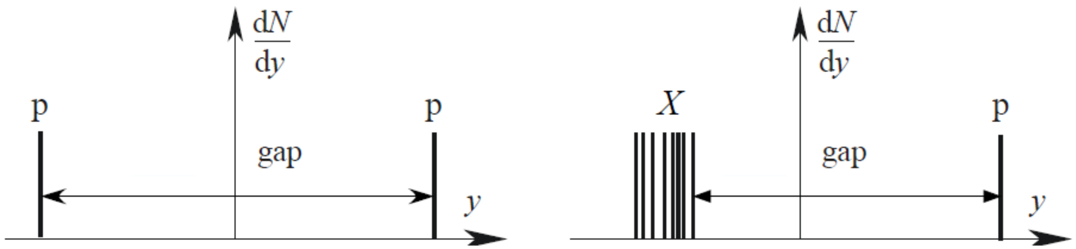

Schematic rapidity distribution of outgoing particles in pp elastic scattering and in pp single diffractive dissociation

Elastic pp $d\sigma_{el}/dt$ measurements at medium and high |t|

E. Nagy et al., Nucl. Phys. B 150, 221 (1979)
W. Faissler et al., Phys. Rev. D 23, 33 (1981)

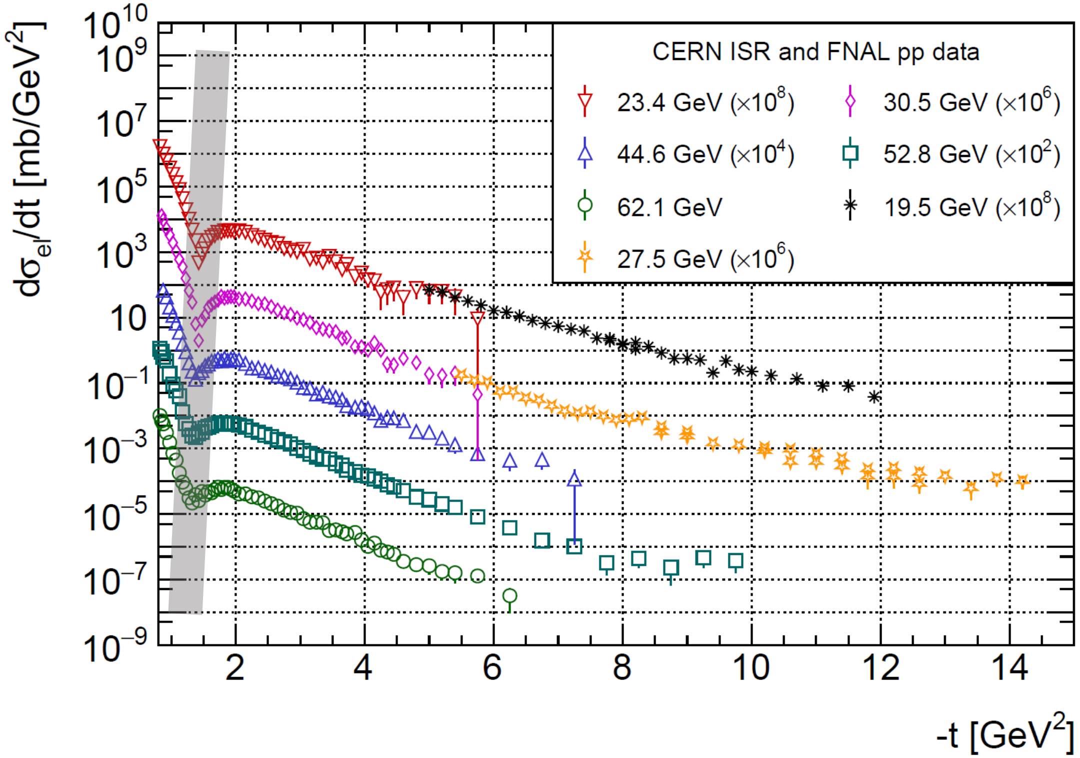

TOTEM Collab., EPL 95:4, 41001 (2011)
TOTEM Collab., Eur. Phys. J. C 79:10, 861 (2019)
TOTEM Collab., Eur. Phys. J. C 80:2, 91 (2020)
TOTEM Collab., Eur. Phys. J. C 82:3, 263 (2022)
TOTEM & D0 Collabs., Phys. Rev. Lett. 127:6, 062003

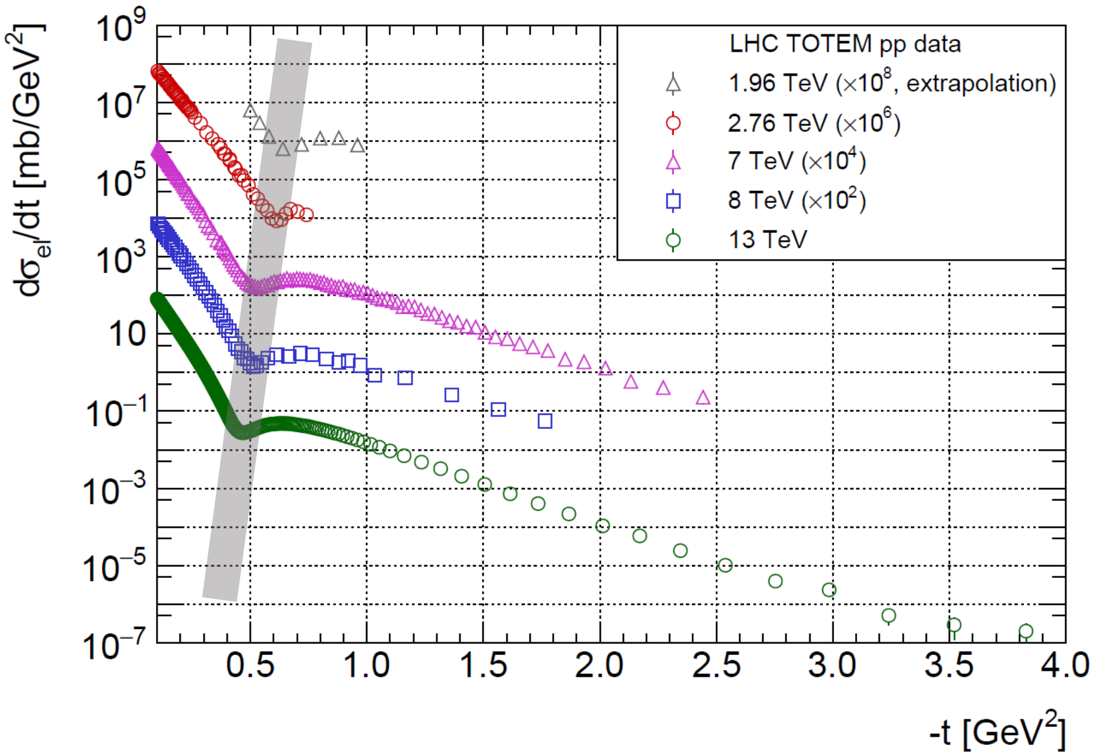

the position of the dip and the bump moves to lower |t| values as the CM energy increases

no secondary dip-bump structures are observed in the |t|range measured up to now

Dipole Regge model

L. L. Jenkovszky and A. N. Wall, Czech. J. Phys. B26, 447 (1976)
L. L. Jenkovszky, Fortsch. Phys.34, 791 (1986)

- basic assumptions:
  - the asymptotic behaviour of the scattering amplitude $A(s,t)$ is determined by an isolated j-plane pole of the second order (dipole)
  - the residue at the pole is independent of t, t-dependence enters only through the trajectory
- the partial wave amplitude is obtained as a derivative of a simple pole:

$$a_j(t) \equiv a(j,t) = \frac{d}{d\alpha(t)}\left[\frac{\beta(j)}{j-\alpha(t)}\right] = \frac{\beta(j)}{[j-\alpha(t)]^2}$$

- **the dipole scattering amplitude is obtained as a derivative of a simple pole scattering amplitude:**

$$\mathrm{A}^{\mathrm{DP}}(s,\alpha) = \frac{d}{d\alpha}\mathrm{A}^{\mathrm{SP}}(s,\alpha) = e^{-\frac{i\pi\alpha}{2}}\left(\frac{s}{s_0}\right)^{\alpha}\left[G'(\alpha) + \left(L - \frac{i\pi}{2}\right)G(\alpha)\right]$$

$$\mathrm{A}^{\mathrm{SP}}(s,\alpha) = e^{-\frac{i\pi\alpha}{2}}G(\alpha)\left(\frac{s}{s_0}\right)^{\alpha}$$

$$\alpha = \alpha(t)$$

$$L \equiv ln\frac{s}{s_0}$$

Dipole Regge model

L. L. Jenkovszky and A. N. Wall, Czech. J. Phys. B26, 447 (1976)
L. L. Jenkovszky, Fortsch. Phys.34, 791 (1986)

$$A^{DP}(s,\alpha) = e^{-\frac{i\pi\alpha}{2}} \left(\frac{s}{s_0}\right)^{\alpha} \left[G'(\alpha) + \left(L - \frac{i\pi}{2}\right) G(\alpha)\right]$$

- motivated by the shape of the diffraction cone (exponential decrease), the paramterization of $G'(\alpha)$ is:

$$G'(\alpha) = a e^{b[\alpha - 1]}$$

- $G(\alpha)$ is obtained by by integrating $G'(\alpha)$:

$$G(\alpha) = \int G'(\alpha) d\alpha = a\left(\frac{e^{b[\alpha-1]}}{b} - \gamma\right)$$

- introducing that $\varepsilon = \gamma b$ the amplitude can be rewritten as:

$$A^{DP}(s,t) = i\frac{a}{b}\left(\frac{s}{s_0}\right)^{\alpha(t=0)} e^{-\frac{i\pi}{2}(\alpha(t=0)-1)} \left[r_1^2(s) e^{r_1^2(s)[\alpha(t)-1]} - \varepsilon\, r_2^2(s) e^{r_2^2(s)[\alpha(t)-1]}\right]$$

$$r_1^2(s) = b + L(s) - i\pi/2 \qquad r_2^2(s) = L(s) - i\pi/2$$

Model for elastic pp and $\bar{p}p$ scattering amplitude

$$A(s,t)^{\bar{p}p}_{pp} = A^{DP}_{P}(s,t) + A^{SP}_{f}(s,t) \pm [A^{DP}_{O}(s,t) + A^{SP}_{\omega}(s,t)]$$

- **the dipole pomeron and odderon amplitudes are:**

$$A^{DP}_{P}(s,t) = e^{-\frac{i\pi\alpha_P(t)}{2}}\left(\frac{s}{s_{0P}}\right)^{\alpha_P}\left[G'_P(t) + \left(L_P(s) - \frac{i\pi}{2}\right)G_P(t)\right]$$

$$A^{DP}_{O}(s,t) = -iA^{DP}_{P\to O}(s,t)$$

(with free parameters labeled by "O")

$$G'_P(t) = a_P e^{b_P[\alpha(t)-1]}$$

$$G_P(t) = a_P\left(e^{b_P[\alpha_P(t)-1]}/b_P - \gamma_P\right)$$

$$L_P(s) = \ln\frac{s}{s_{0P}}$$

$$\alpha_P(t) = 1 + \delta_P + \alpha'_P t$$

- **the simple pole f and ω reggeon amplitudes are:**

$$\mathbf{A_f}(s,t) = a_f e^{-\frac{i\pi\alpha_f(t)}{2}}(s/s_0)^{\alpha_f(t)} e^{b_f t}$$

$$\mathbf{A_\omega}(s,t) = i\mathbf{A_{f\to\omega}}(s,t)$$

$$\alpha_f(t) = \alpha^0_f + \alpha'_f t$$

(with free parameters labeled by "ω")

ISR $d\sigma_{el}/dt$ data and the model

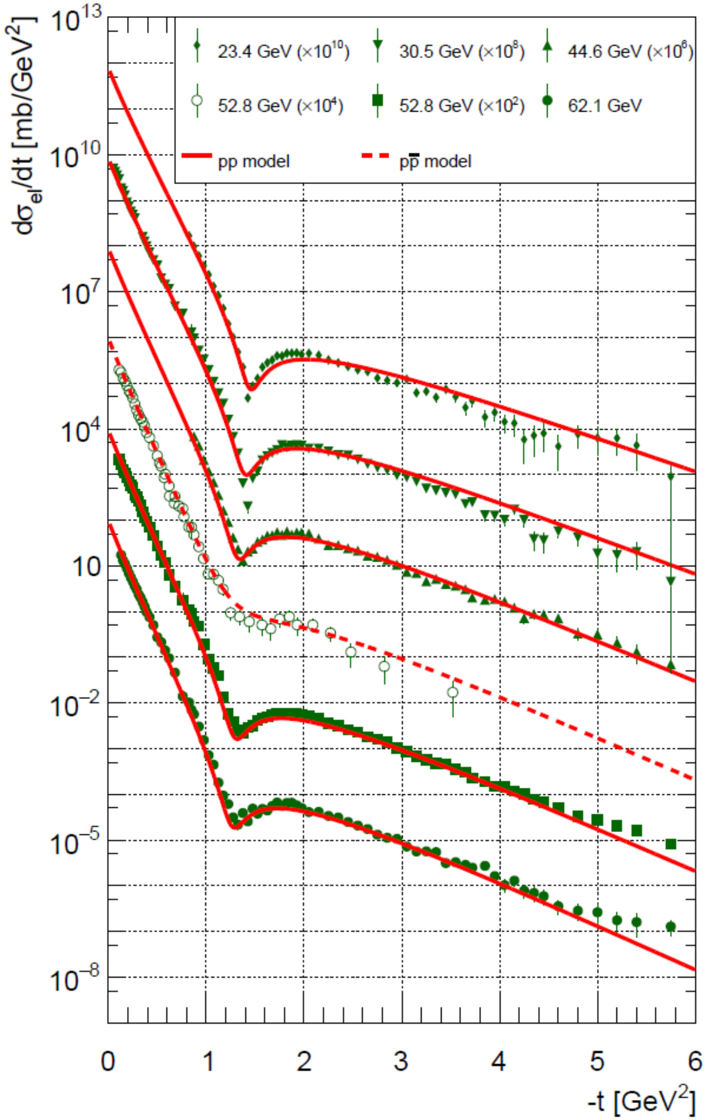

Pomeron	Odderon	f-reggeon	ω-reggeon
$\delta_P = 0.043$	$\delta_O = 0.14$	$\alpha_f^0 = 0.69$	$\alpha_\omega^0 = 0.44$
$\alpha'_P = 0.36$	$\alpha'_O = 0.13$	$\alpha'_f = 0.84$	$\alpha'_\omega = 0.93$
$a_P = 9.10$	$a_O = 0.029$	$a_f = -15.4$	$a_\omega = 9.69$
$b_P = 8.47$	$b_O = 6.96$	$b_f = 4.78$	$b_\omega = 3.5$
$\gamma_P = 0$	$\gamma_O = 0.11$	-	-
$s_{0P} = 2.88$	$s_{0O} = 1$	$s_{0f} = 1$	$s_{0\omega} = 1$

Fit to proton-proton and proton-antiproton differential cross section data at ISR energy region, and to ρ and total cross section data from 5 GeV up to the highest energies

$d\sigma_{el}/dt$ with P and O contribution, ρ and σ_{tot} w/o O

the odderon contribution takes over completely after the bump but at low-|t| the odderon contribution is small

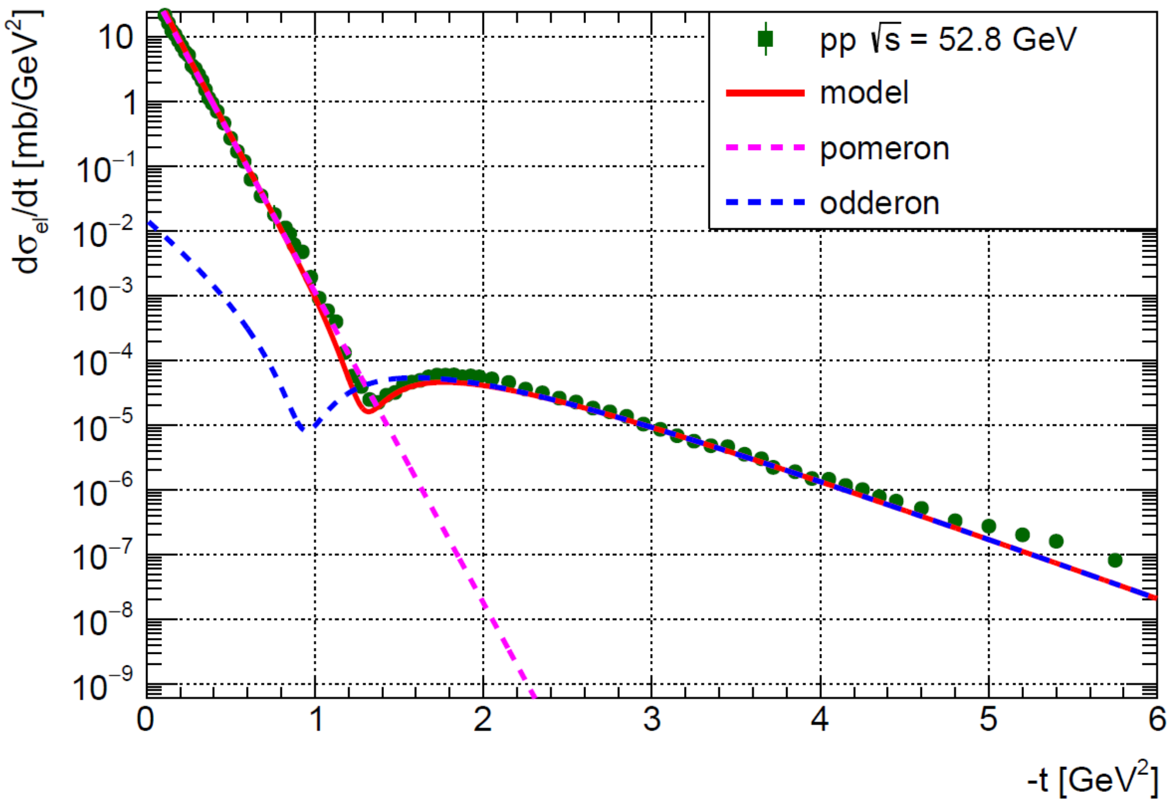

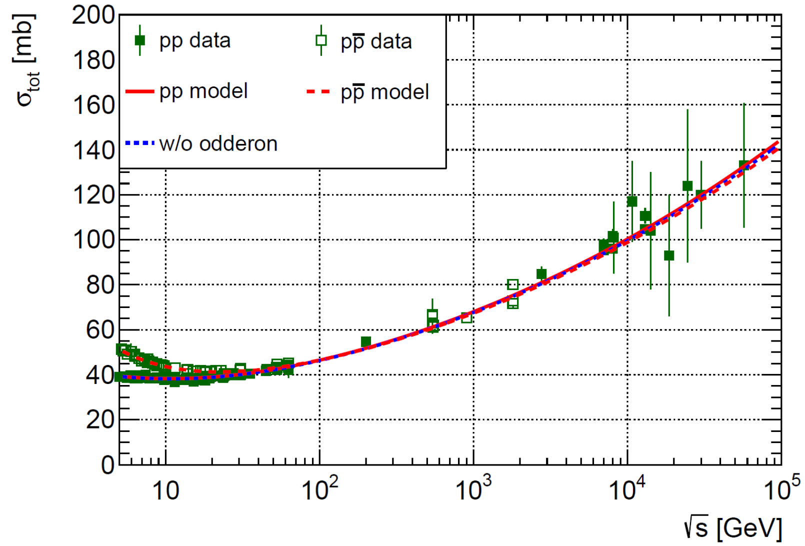

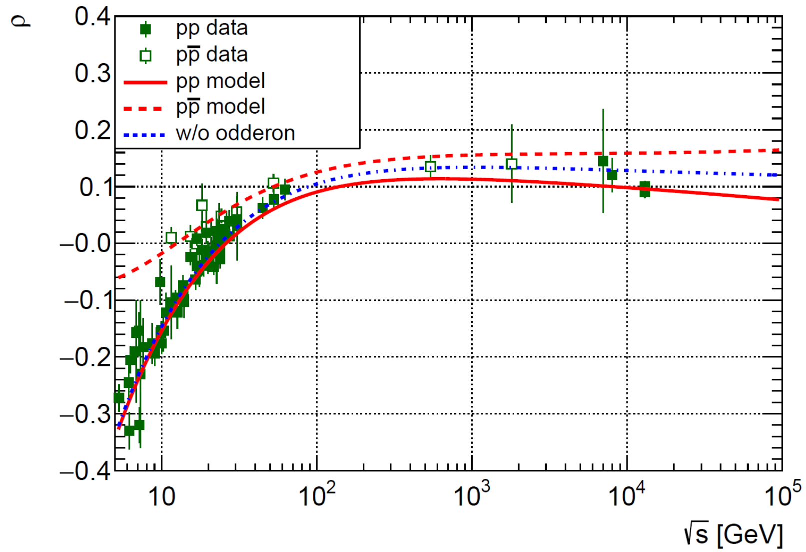

$d\sigma_{el}/dt$ with P and O contribution, ρ and σ_{tot} w/o O

the odderon contribution takes over completely after the bump but at low-|t| the odderon contribution is small

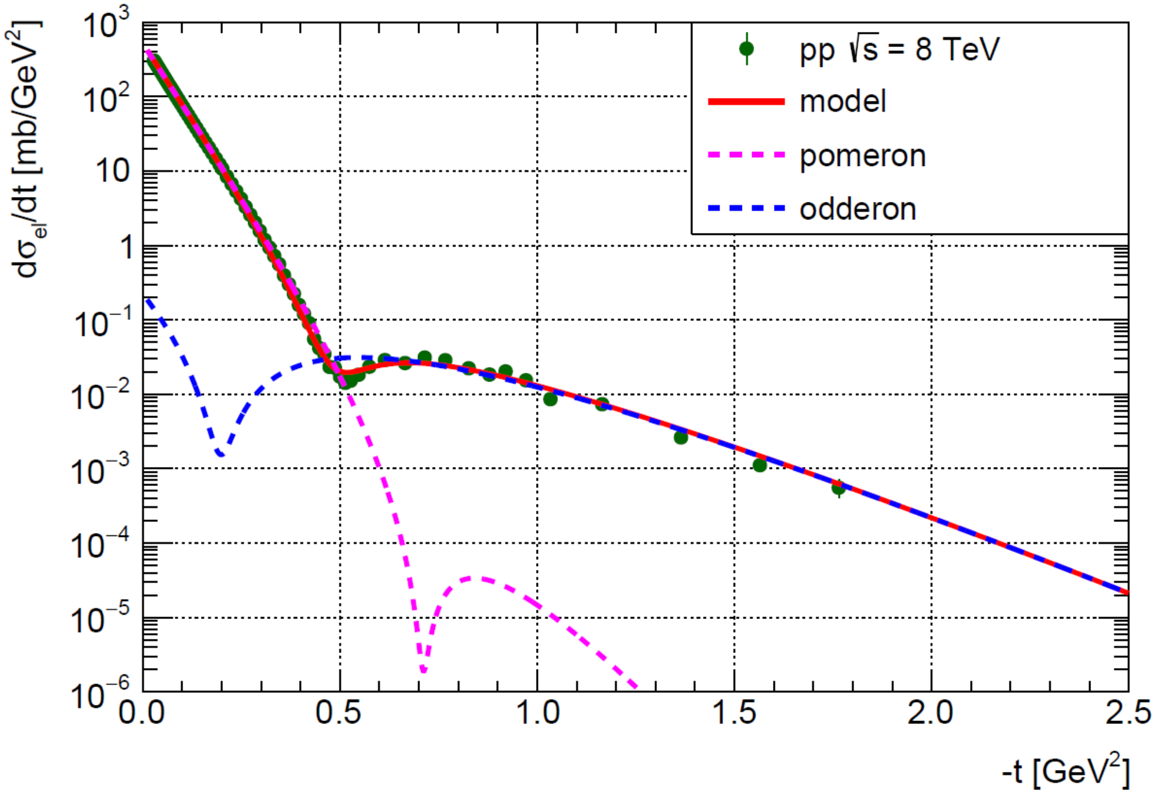

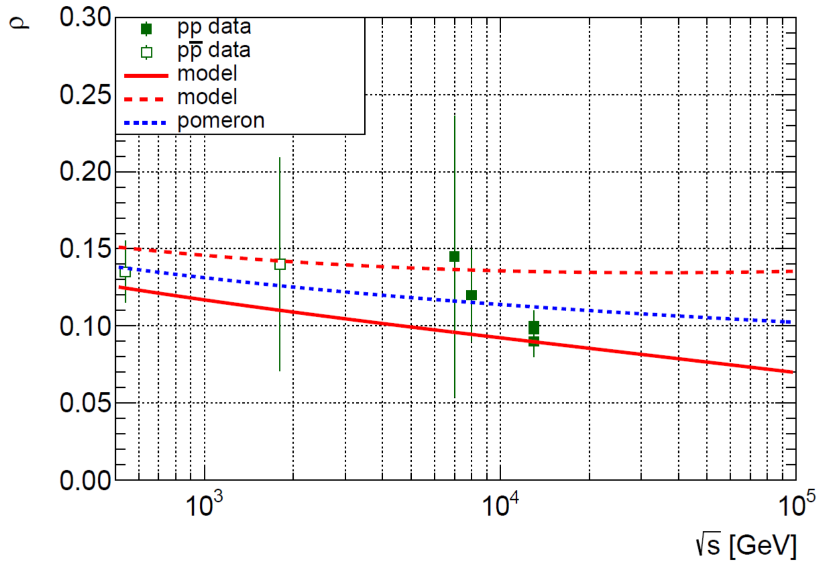

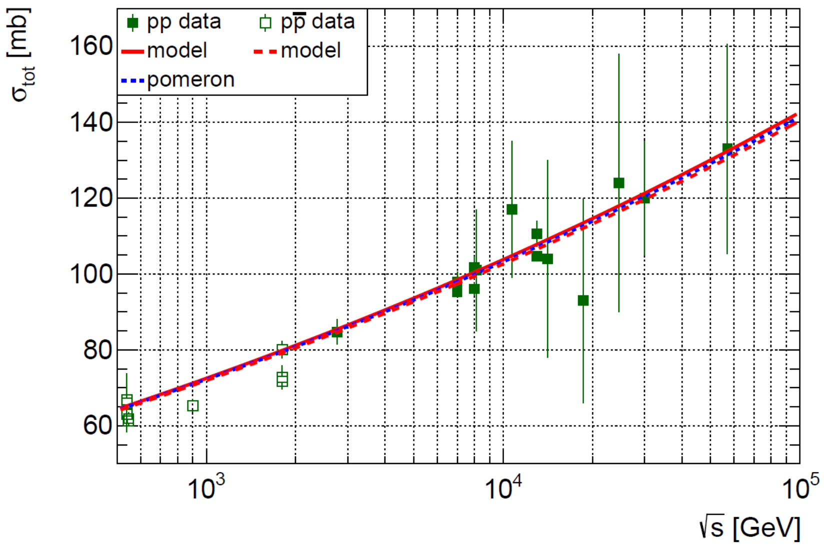

Dip-bump structures in single diffractive dissociation?

- measurements of pp single diffractive dissociation at ISR do not show a dip-bump structure at |t| values where such a structure is observed in elastic pp scattering

  M.G. Albrow et al., Nucl. Phys. B72, 376 (1974)

- it can be explained in a framework of a dipole Regge model in which the dip-bump structure moves to higher |t| values as the value of the slope parameter decreases
- **a dipole odderon+pomeron Regge approach can be used to predict dip-bump structures in pp single diffractive dissociation at LHC energies**

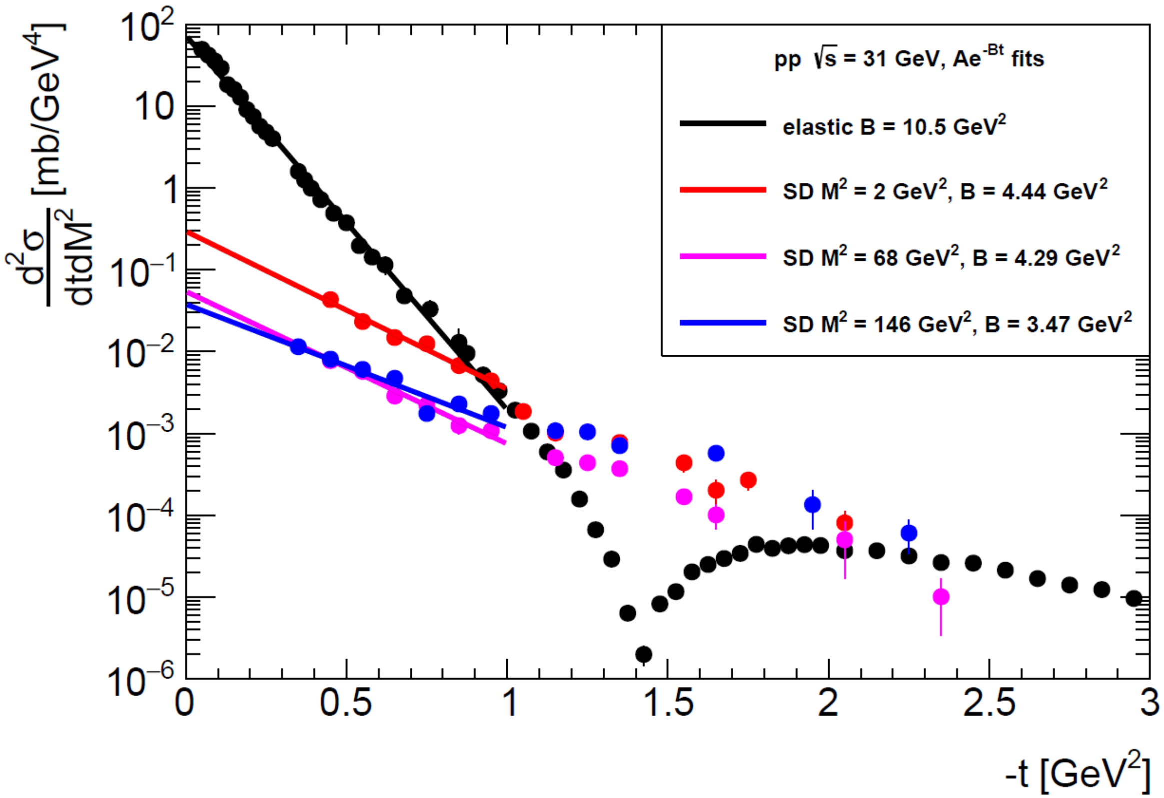

t dependence of the SD process at 8 TeV

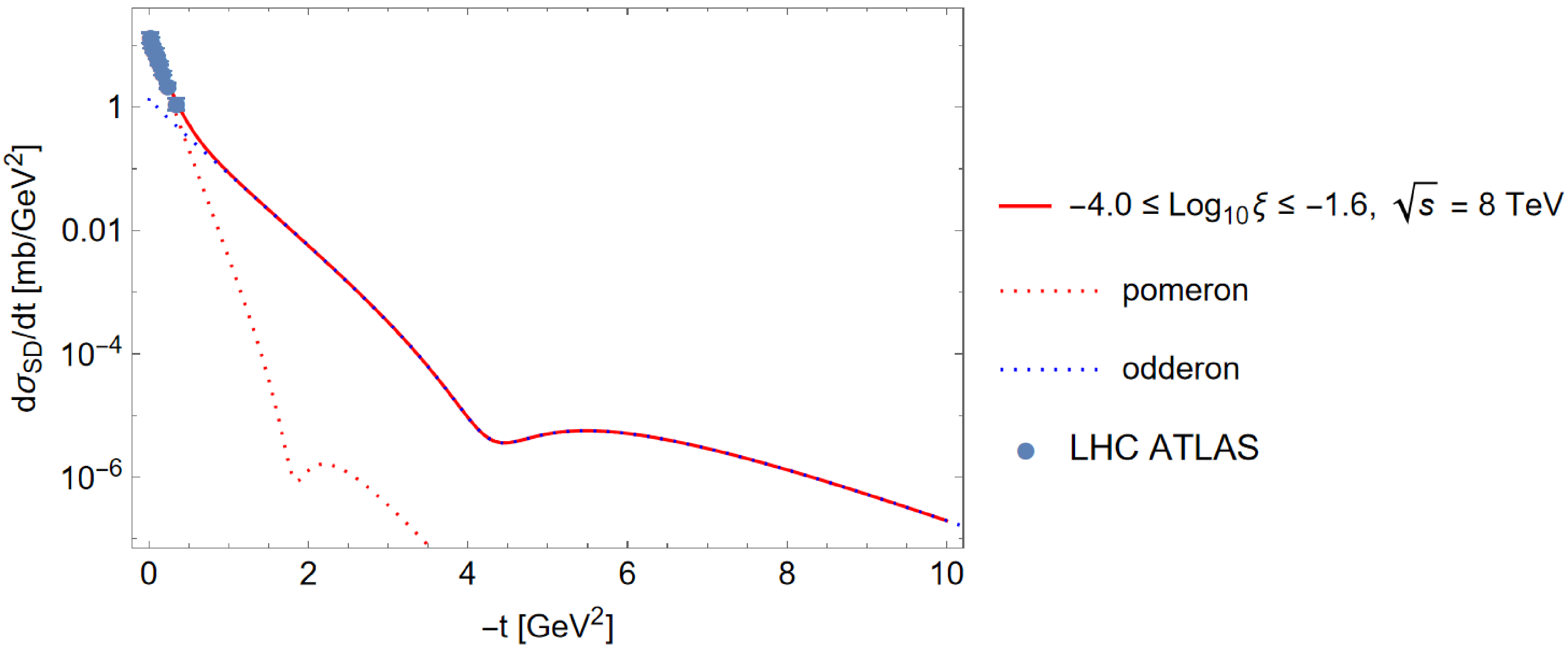

Exclusive soft reactions in high-energy proton-proton collisions

Piotr Lebiedowicz
IFJ PAN, Kraków, Poland

THE HENRYK NIEWODNICZAŃSKI
INSTITUTE OF NUCLEAR PHYSICS
POLISH ACADEMY OF SCIENCES

in collaboration with Otto Nachtmann (Univ. Heidelberg)
and Antoni Szczurek (IFJ PAN)

EMMI Workshop, Forward Physics in ALICE 3
18-20 Oct 2023, Phys. Institute, University Heidelberg, Germany
https://indico.cern.ch/event/1327118/

Pomeron: tensor vs vector

- Tensor pomeron, C = +1 (effective symmetric tensor exchange)

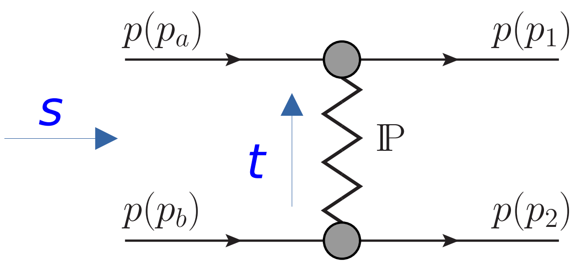

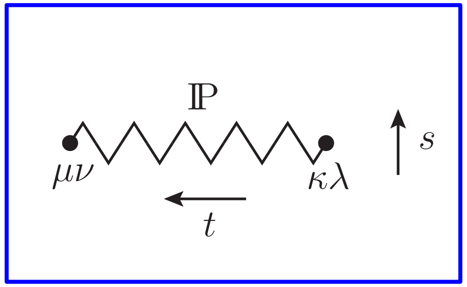

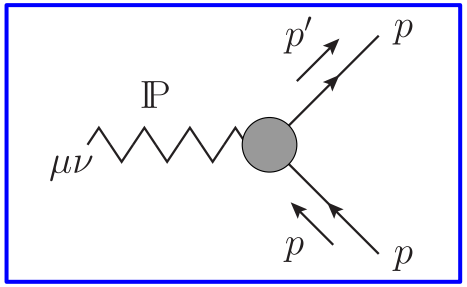

Ewerz, Maniatis, Nachtmann, Ann. Phys. 342 (2014) 31

$$i\Delta^{(\mathbb{P})}_{\mu\nu,\kappa\lambda}(s,t) = \frac{1}{4s}\left(g_{\mu\kappa}g_{\nu\lambda} + g_{\mu\lambda}g_{\nu\kappa} - \frac{1}{2}g_{\mu\nu}g_{\kappa\lambda}\right)(-is\tilde{\alpha}'_{\mathbb{P}})^{\alpha_{\mathbb{P}}(t)-1}$$

$$i\Gamma^{(\mathbb{P}pp)}_{\mu\nu}(p',p) = -i3\beta_{\mathbb{P}pp}F_1(t)\left\{\frac{1}{2}\left[\gamma_\mu(p'+p)_\nu + \gamma_\nu(p'+p)_\mu\right] - \frac{1}{4}g_{\mu\nu}(\not{p}'+\not{p})\right\}$$

$\mathbb{P}$ trajectory : $\alpha_{\mathbb{P}}(t) = \alpha_{\mathbb{P}}(0) + \alpha'_{\mathbb{P}}\,t$ $\left\{ \begin{array}{l} \alpha_{\mathbb{P}}(0) = 1 + \epsilon_{\mathbb{P}} \simeq 1.08 - 1.09 \\ \alpha'_{\mathbb{P}} = 0.25\ \text{GeV}^{-2} \end{array} \right.$

$F_1(t)$: form factor

$\tilde{\alpha}'_{\mathbb{P}}$: scale parameter, $\tilde{\alpha}'_{\mathbb{P}} = 0.25\ \text{GeV}^{-2}$

$\beta_{\mathbb{P}pp}$: coupling parameter, $\beta_{\mathbb{P}pp} = 1.87\ \text{GeV}^{-1}$

"Pomeron Physics and QCD", Donnachie, Dosch, Landshoff, Nachtmann, CUP, 2002

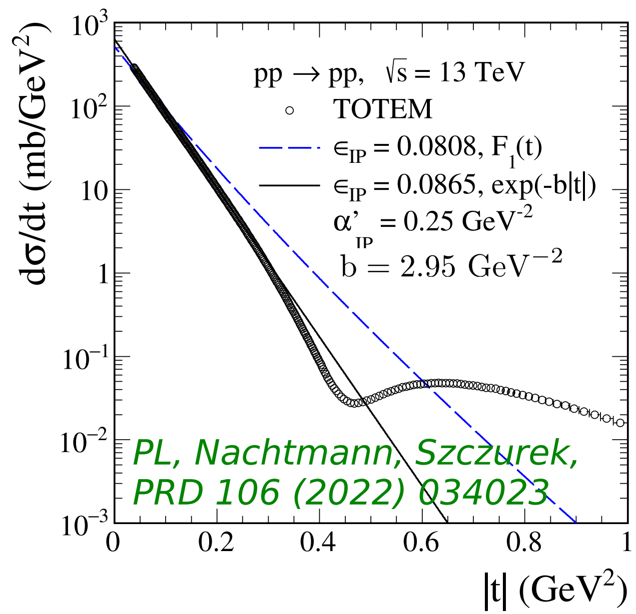

- Vector pomeron, C = -1 (Donnachie-Landshoff pomeron)

$$i\Delta^{(\mathbb{P}_V)}_{\mu\nu}(s,t) = \frac{1}{M_0^2}g_{\mu\nu}(-is\tilde{\alpha}'_{\mathbb{P}})^{\alpha_{\mathbb{P}}(t)-1}$$

$$i\Gamma^{(\mathbb{P}_V pp)}_{\mu}(p',p) = -i3\beta_{\mathbb{P}pp}F_1(t)M_0\gamma_\mu\,, \qquad M_0 = 1\ \text{GeV}$$

Central Exclusive Production (CEP)

At high energies double pomeron exchange (DPE) is dominant production mechanism of resonances.

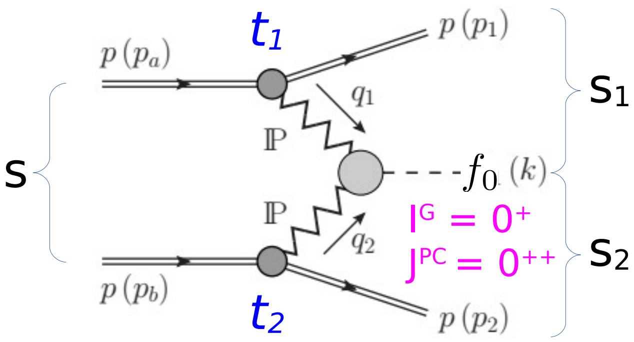

$$p\,(p_a\,,\,\lambda_a) + p\,(p_b\,,\,\lambda_b) \to p\,(p_1\,,\,\lambda_1) + f_0\,(k) + p\,(p_2\,,\,\lambda_2), \quad \lambda_i = \pm 1/2$$

The Born amplitude is written in terms of the the effective pomeron-proton vertex function, pomeron propagator, and the pomeron-pomeron-f_0 vertex:

$$\mathcal{M}^{\mathrm{Born}}_{\lambda_a\lambda_b\to\lambda_1\lambda_2 f_0} = (-i)\bar{u}(p_1,\lambda_1)i\Gamma^{(I\!\!Ppp)}_{\mu_1\nu_1}(p_1,p_a)u(p_a,\lambda_a)$$
$$\times i\Delta^{(I\!\!P)\,\mu_1\nu_1,\alpha_1\beta_1}(s_1,t_1)\,i\Gamma^{(I\!\!PI\!\!Pf_0)}_{\alpha_1\beta_1,\alpha_2\beta_2}(q_1,q_2)\,i\Delta^{(I\!\!P)\,\alpha_2\beta_2,\mu_2\nu_2}(s_2,t_2)$$
$$\times\bar{u}(p_2,\lambda_2)i\Gamma^{(I\!\!Ppp)}_{\mu_2\nu_2}(p_2,p_b)u(p_b,\lambda_b)$$

$$q_1 = p_a - p_1, \quad q_2 = p_b - p_2, \quad k = q_1 + q_2$$
$$t_1 = q_1^2, \quad t_2 = q_2^2, \quad m^2_{f_1} = k^2$$
$$s = (p_a + p_b)^2 = (p_1 + p_2 + k)^2\,, \ \text{c.m. energy squared}$$
$$s_1 = (p_1 + k)^2, \quad s_2 = (p_2 + k)^2$$

- To give the full physical amplitude we should include absorptive corrections to the Born amplitude:

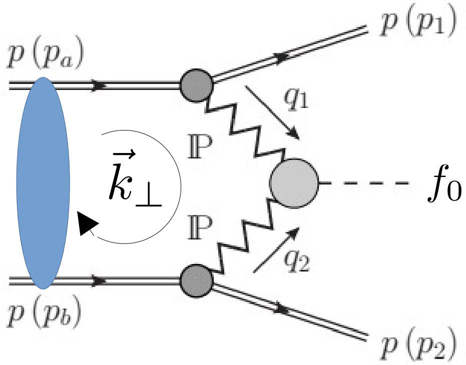

$$\mathcal{M}_{pp\to ppf_0} = \mathcal{M}^{\mathrm{Born}}_{pp\to ppf_0} + \mathcal{M}^{pp-\mathrm{rescattering}}_{pp\to ppf_0}$$

$$\mathcal{M}^{pp-\mathrm{rescattering}}_{pp\to ppf_0}(s,\vec{p}_{1\perp},\vec{p}_{2\perp}) = \frac{i}{8\pi^2 s}\int d^2\vec{k}_\perp \mathcal{M}^{\mathrm{Born}}_{pp\to ppf_0}(s,\vec{p}_{1\perp}-\vec{k}_\perp,\vec{p}_{2\perp}+\vec{k}_\perp)$$
$$\times\mathcal{M}^{I\!\!P-\mathrm{exchange}}_{pp\to pp}(s,-\vec{k}^2_\perp)$$

where $\vec{k}_\perp$ is the transverse momentum carried around the loop

CEP, *IP-IP-M* couplings

We consider the annihilation of two “pomeron particles” of spin 2 giving a meson *M*, in the rest system of *M*,

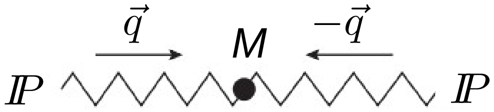

l – orbital angular momentum
S – total $I\!P I\!P$ spin, we have $S \in \{0, 1, 2, 3, 4\}$
J – total angular momentum (spin of produced meson)
P – parity of meson
and Bose symmetry requires $l - S$ to be even

l	S	$\lvert l-S\rvert \leqslant J \leqslant l+S$	$P = (-1)^l$
0	0	0	+
	2	2	
	4	4	
1	1	0, 1, 2	−
	3	2, 3, 4	
2	0	2	+
	2	0,1,2,3,4	
	4	2,3,4,5,6	
3	1	2,3,4	−
	3	0,1,2,3,4,5,6	
4	0	4	+
	2	2,3,4,5,6	
	4	0,1,2,3,4,5,6,7,8	
5	1	4.5.6	−
	3	2,3,4,5,6,7,8	
6	0	6	+
	2	4,5,6,7,8	
	4	2,3,4,5,6,7,8,9,10	

For each value of (ℓ,S) we can construct a covariant Lagrangian density coupling the field operator for the meson χ to the pomeron fields $I\!P_{\mu\nu}$.

The lowest (ℓ,S) term for a scalar meson $J^{PC} = 0^{++}$ is (0,0).

The Lagrangian for a scalar meson corresponding to (ℓ,S) = (0,0) is

$$\mathcal{L}'_{I\!P I\!P M}(x) = M_0\, g'_{I\!P I\!P M}\, I\!P_{\mu\nu}(x) I\!P^{\mu\nu}(x)\chi(x)$$

with $M_0 \equiv 1$ GeV, and $g'_{I\!P I\!P M}$ the dimensionless coupling constant.

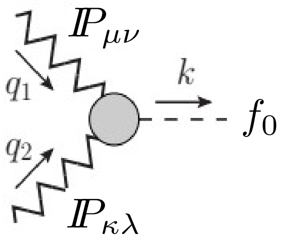

The ‘bare’ vertex obtained from $\mathcal{L}'_{I\!P I\!P M}$ reads

$$i\Gamma'^{(I\!P I\!P f_0)}_{\mu\nu,\kappa\lambda} = i\, g'_{I\!P I\!P f_0} M_0 \left(g_{\mu\kappa} g_{\nu\lambda} + g_{\mu\lambda} g_{\nu\kappa} - \frac{1}{2} g_{\mu\nu} g_{\kappa\lambda} \right)$$

The ‘bare’ vertex for (ℓ,S) = (2,2) obtained from $\mathcal{L}''_{I\!P I\!P M}$ is

$$i\Gamma''^{(I\!P I\!P f_0)}_{\mu\nu,\kappa\lambda}(q_1, q_2) = i\,\frac{g''_{I\!P I\!P f_0}}{2M_0}\,[q_{1\kappa} q_{2\mu} g_{\nu\lambda} + q_{1\kappa} q_{2\nu} g_{\mu\lambda} + q_{1\lambda} q_{2\mu} g_{\nu\kappa} + q_{1\lambda} q_{2\nu} g_{\mu\kappa} - 2(q_1 \cdot q_2)(g_{\mu\kappa} g_{\nu\lambda} + g_{\nu\kappa} g_{\mu\lambda})]$$

In CEP reaction we must take into account that hadrons are extended objects → we introduce form factor

$$i\Gamma^{(I\!P I\!P f_0)}_{\mu\nu,\kappa\lambda}(q_1, q_2) = \left(i\Gamma'^{(I\!P I\!P f_0)}_{\mu\nu,\kappa\lambda} + i\Gamma''^{(I\!P I\!P f_0)}_{\mu\nu,\kappa\lambda}(q_1, q_2) + i\Gamma'''^{(I\!P I\!P f_0)}_{\mu\nu,\kappa\lambda}(q_1, q_2) \right) F_{I\!P I\!P f_0}(q_1^2, q_2^2, k^2)$$

The values of the coupling constants (g', g'', g''') are not known as they are of nonperturbative origin and have to be determined from experiment. In general more than one (ℓ,S) coupling term is needed for the description of experimental results.

CEP, *IP-IP-M* couplings

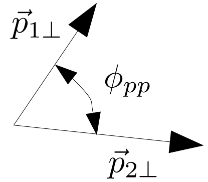

WA102 Collaboration observed that:

- there is an important qualitative difference in the ϕ_{pp} distribution:
  - → $f_0(1370)$, $f_2(1270)$ and $f'_2(1525)$ peak as $\phi_{pp} \to \pi$
  - → $f_0(980)$, $f_0(1500)$, $f_0(1710)$ peak at $\phi_{pp} \to 0$
- the "undisputed" $q\bar{q}$ states (i.e. η, η', $f_1(1285)$, $f_2(1270)$, $f'_2(1525)$) are suppressed when $dP_t \to 0$, whereas the states which could have a non-$q\bar{q}$ or a large 'gluonic component' *e.g.* $f_0(1500)$, $f_0(1710)$, $f_2(1950)$, $f_2(2340)$ (potential glueballs) are prominent

"glueball filter variable" F. Close
$$dP_t = |d\vec{P}_t| = |\vec{q}_{1\perp} - \vec{q}_{2\perp}| = |\vec{p}_{2\perp} - \vec{p}_{1\perp}|$$

Example: *f₀*(980) *[PL, Nachtmann, Szczurek, Annals Phys. 344 (2014) 301; PRD98 (2018) 014001]*

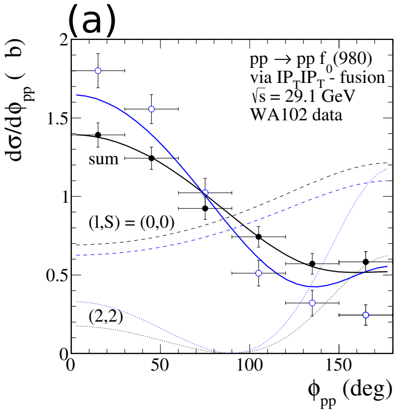

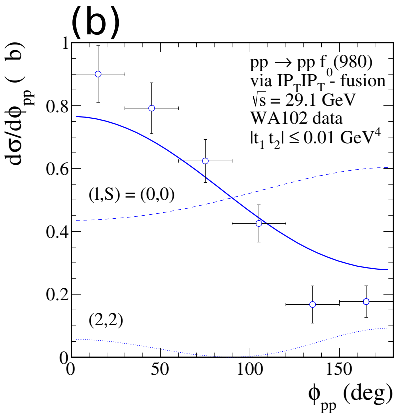

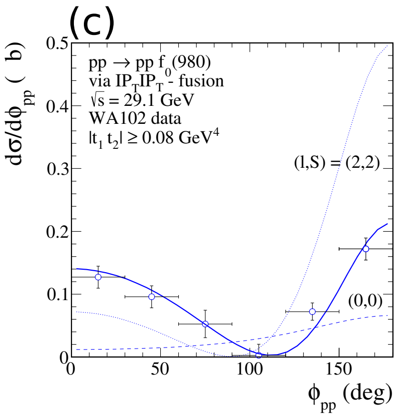

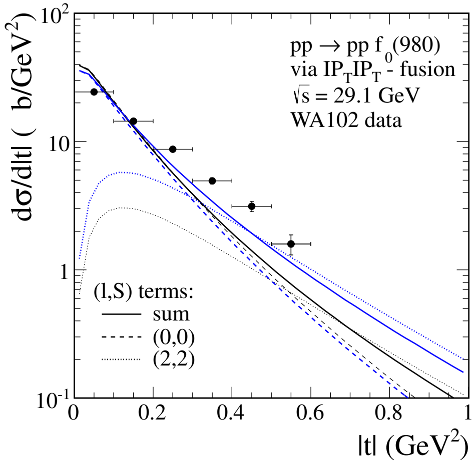

Example: *f₀*(1710)

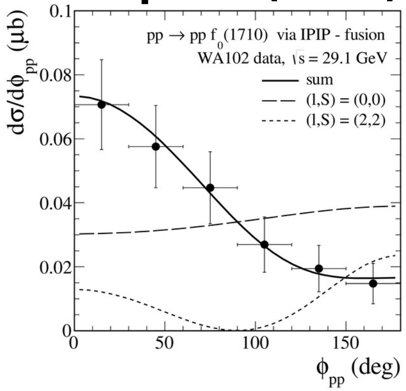

- for $f_0(980)$ both $(\ell,S) = (0,0)$ and $(2,2)$ contributions are necessary and the same for $f_0(1500)$ and $f_0(1710)$, but for $f_0(1370)$ only $(\ell,S) = (0,0)$
- at $|t| \to 0$ the (2,2) component vanishes
- also theoretical predictions of dP_t seem to be qualitatively consistent with data
- at low energies (WA102) the socondary exchanges (f2-reggeon) may also play an important role

Our results and WA102 data (black points [1] and blue points [2]) have been normalised to the mean value of the total cross sections given in [3]. The WA102 data in panels (b) and (c) are obtained from [2] with the normalisation calculated in the model themselves for lack of experimental information.

[1] WA102 Collaboration, D. Barberis et al., PLB 462 (1999) 462; [2] PLB 467 (1999) 165; [3] A. Kirk, PLB 489 (2000) 29

$pp \to pp\ \pi^+\pi^-$

PRELIMINARY

STAR data JHEP 07 (2020) 178

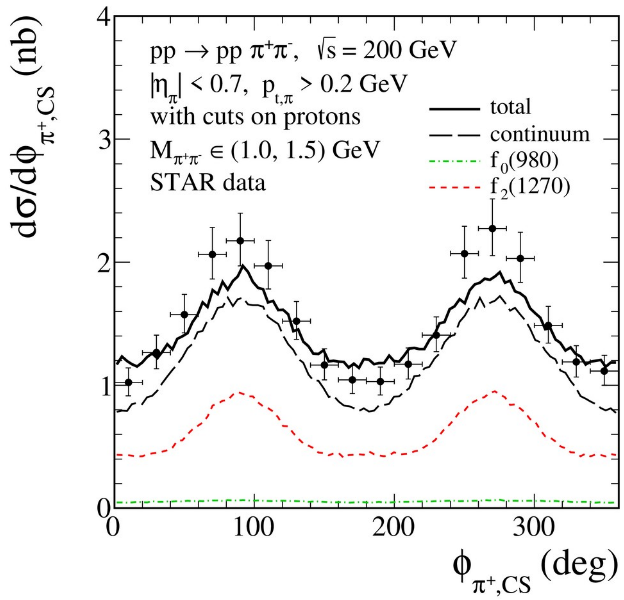

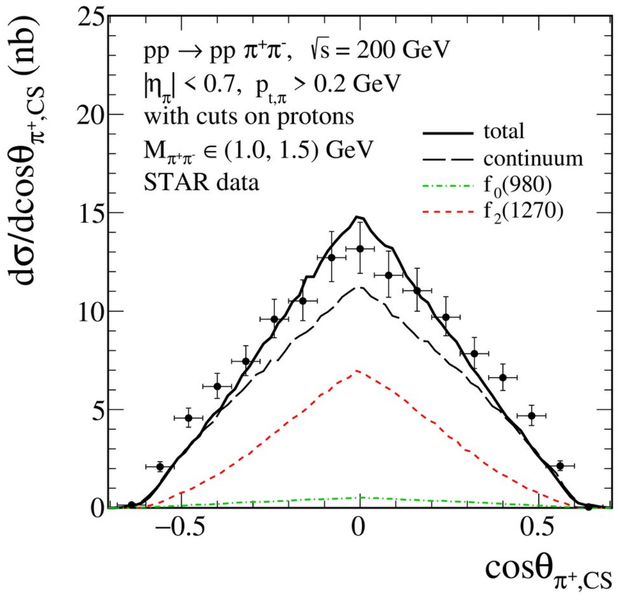

with cuts on protons

$(p_x + 0.3\ \text{GeV})^2 + p_y^2 < 0.25\ \text{GeV}^2$

$0.2\ \text{GeV} < |p_y| < 0.4\ \text{GeV}$

$p_x > -0.2\ \text{GeV}$

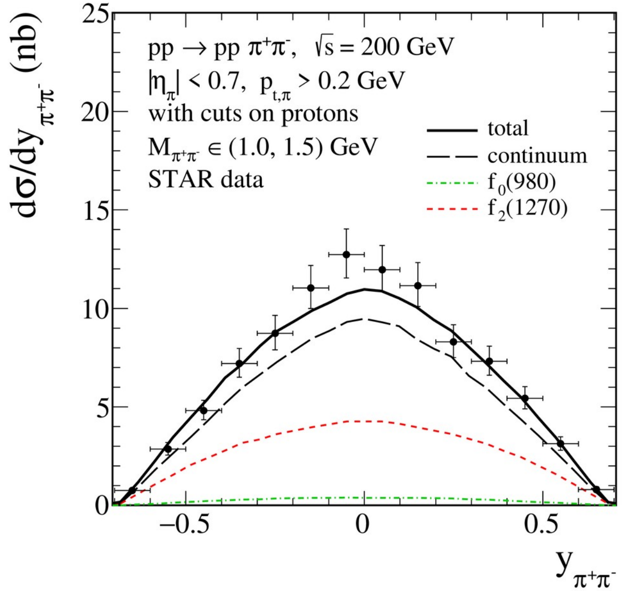

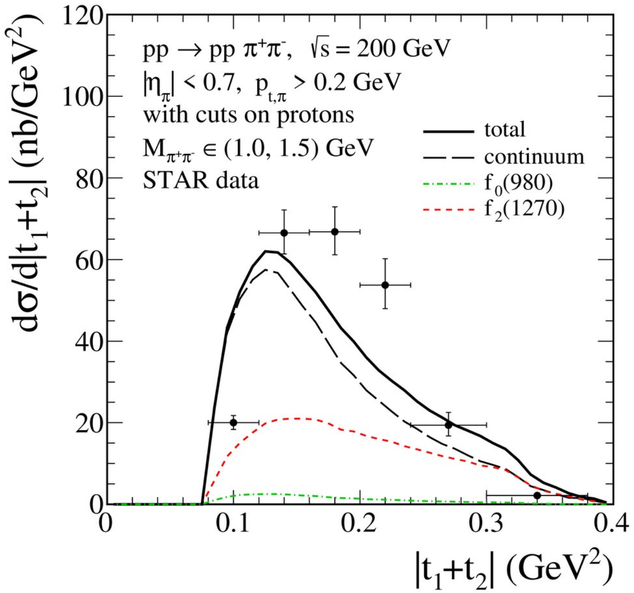

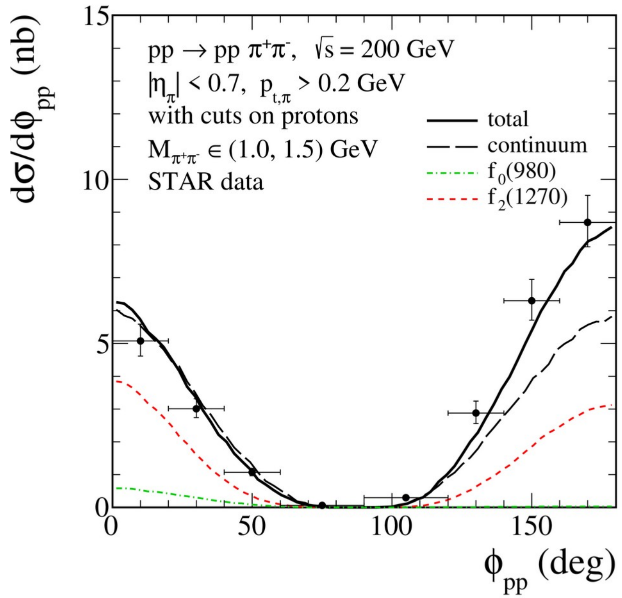

Probing gluon saturation in heavy-ion collisions at forward rapidities

Georg Wolschin

Heidelberg University

Institut für Theoretische Physik

Philosophenweg 16

D-69120 Heidelberg

Topics

1. Introduction

2. Net-baryon transport (“stopping”) in heavy-ion collisions

   2.1 Nonequilibrium-statistical stopping model

   2.2 Energy and time dependence of net-baryon transport, Role of gluon saturation

3. Limiting-fragmentation scaling in stopping?

   3.1 Scaling in baryon stopping: Limiting-fragmentation vs. geometric scaling

   3.2 Comparison with SPS and RHIC stopping data, predictions at LHC energies

4. Summary and Conclusion

2. Net-baryon transport ("stopping") in heavy-ion collisions

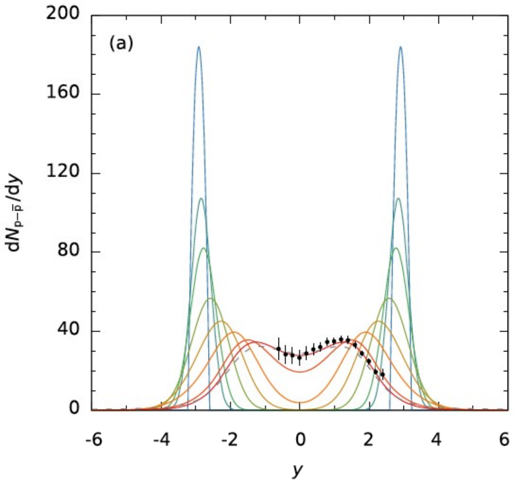

Net-proton rapidity distribution
for central Pb-Pb at

- Investigate the flow of valence quarks (with baryon number 1/3) by studying the time-dependence of net-baryon transport ("stopping"), primarily at forward rapidities

- I do not follow here possible traces of net baryon number in the gluon field through baryon junctions, which could also lead to baryon asymmetry, in the midrapidity region: See the talk of Chun Yuen Tsang

- Concentrate on the baryon number associated with the incoming valence quarks in the forward-rapidity region, and investigate its time-dependence from the initial Fermi gas towards the final color-glass condensate (CGC) stopping distribution

- Main model assumption: The net-baryon transport at forward rapidities / small scattering angles is dominated by interactions of valence quarks with soft gluons in the other nucleus

- This allows to study the effect of gluon saturation on the net-baryon distributions at forward rapidities (small scattering angles)

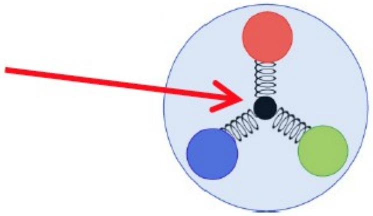

Quarks connected to
a stopped junction
are sea quarks

More pronounced effect of gluon saturation in stopping expected at LHC energies and forward rapidities, but no data available yet:

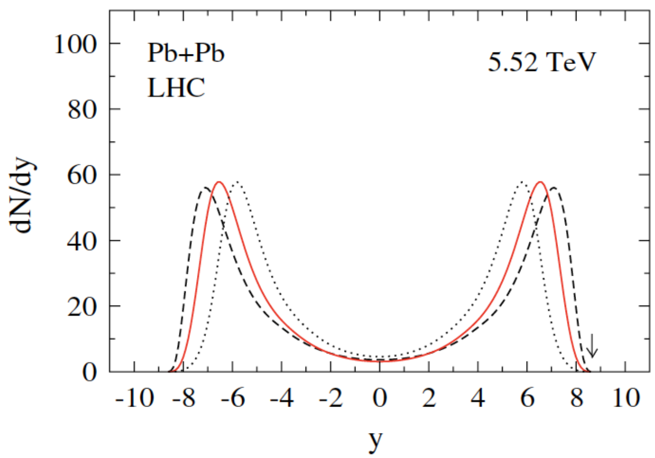

λ = - - 0, — 0.15, ··· 0.3:

Stopping peak position depends on the gluon saturation scale

Y. Mehtar-Tani, G. Wolschin, PRL 102, 182301 (2009)

=> Net-baryon (proton) LHC data at forward rapidity needed

Mean rapidity loss at the stopping-peak position:
Dependence on the gluon saturation-scale exponent λ

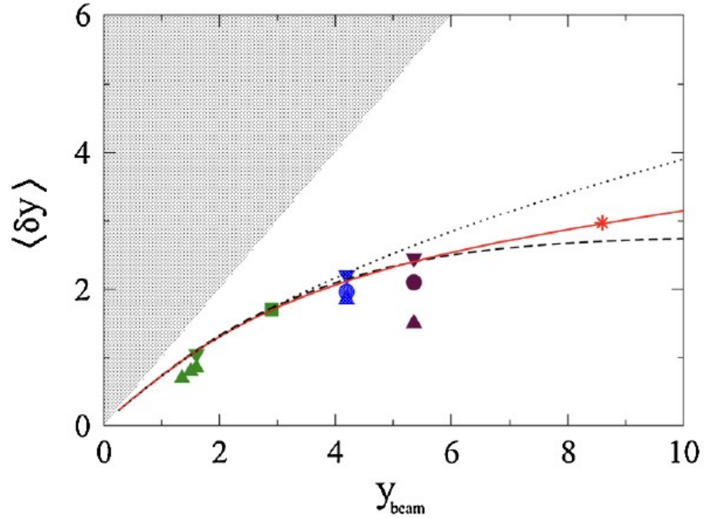

$$\langle \delta y \rangle = \frac{\lambda}{1+\lambda} y_{\text{beam}} + \text{const.}$$ for $y_{beam} > 5$

- ▲▼ AGS Au-Au data (E917: 3.4, 3.9, 4.5 GeV; E802: 4.7 GeV)
- ■ SPS Pb-Pb data (NA49: 17.2 GeV)
- ● RHIC Au-Au data (BRAHMS: 62.4 GeV)
- ● RHIC Au-Au data (BRAHMS: 200 GeV)
- * LHC Pb-Pb prediction ($\sqrt{s_{NN}}$=5.52 TeV)